

Research on the performance of indoor visible light Non-DC-Biased OFDM system based on color/frequency/space three-dimension resources multiplexing

Deng Lijun, Fan Yangyu

(School of Electronics and Information, Northwestern Polytechnical University, Xi'an 710048, China)

Abstract: In this paper, a novel orthogonal frequency division multiplexing (OFDM)-based indoor visible light communication (VLC) system was proposed that can provide a high reliability transmission performance while maintaining ambient light stability by using multicolor LEDs. This solution combines Spatial Modulation (SM) and Metameric Modulation (MM) with OFDM-VLC communication system. Along with all of the promising advantages of OFDM, SM and MM, the proposed system will be applicable for high-speed indoor white communication. Through the simulation results, it is known that the proposed indoor visible light transmission system has significant advantages over DC-biased Optical OFDM (DCO-OFDM) and Asymmetrically Clipped Optical OFDM(ACO-OFDM). Moreover, it is robust to the nonlinear distortion caused by a large peak-to-average power ratio (PAPR) of OFDM signal in comparison with other NDC-OFDM VLC transmission systems, and hardly generate intensity fluctuation.

Key words: indoor visible-light communication; optical OFDM; spatial modulation; metameric modulation

CLC Number: TN929.12 **Document code:** A **DOI:** 10.3788/IRLA201645.0722002

色/频/空三维资源复用的室内可见光非直流偏置 OFDM 系统性能研究

邓莉君, 樊养余

(西北工业大学 电子信息学院, 陕西 西安 710048)

摘要: 提出一种新的室内可见光非直流偏置正交频分 (Non-DC-Biased Orthogonal Frequency Division Multiplexing, NDC-OFDM) 复用系统, 该系统采用多个颜色 LEDs 作为光源, 在保证高传输可靠性的同时可以维持环境光的稳定。将空间调制和同色异谱调制结合并应用到室内可见光 OFDM 通信系统中得到一种新的适用于室内可见光通信系统的 NDC-OFDM 传输方案, 该方案具有 OFDM、空间调制和同色异谱调制的优势, 适用于高速室内白光通信系统。仿真结果表明所提出的 NDC-OFDM 室内可见光传输系统与传统的直流偏置光 OFDM(DC-biased Optical OFDM)和非对称限幅光 OFDM (Asymmetrically Clipped Optical OFDM)相比具有更好的优势, 并且与其它 NDC-OFDM 室内可见光传

收稿日期: 2015-11-05; 修订日期: 2015-12-03

基金项目: 国家自然科学基金(61377080); 国家自然科学基金青年基金(61405157)

作者简介: 邓莉君(1986-), 女, 博士生, 主要从事室内可见光基础理论与关键技术等方面的研究。Email: denglijun1231@163.com

导师简介: 樊养余(1960-), 男, 教授, 博士生导师, 主要从事波束形成与波达方向估计, 空间、大气光通信, 室内、可见光通信、水下光通信等方面的研究。Email: Fan_yangyu@nwpu.edu.cn

输方案相比, 对于 OFDM 信号高峰均功率比引起的光信号非线性畸变问题, 本文提出的多色 LEDs NDC-OFDM 室内可见光传输方案除了具有更好的鲁棒性外, 还不会产生光强度波动。

关键词: 室内可见光通信; 光 OFDM; 空间调制; 同色异谱调制

0 Introduction

In indoor wireless communication, visible light communication(VLC) systems has gained a lot of interest thanks to the wide optical bandwidth that can support high speed data rates in our daily lives compared to RF and infrared based systems. VLC is an optical wireless communication (OWC) technology that can transmit information through a solid state light source (e.g., LED, LASER) with its main functionality such as illumination and visual display. The inherent advantages of VLC is that it has aesthetically pleasing, an unregulated huge bandwidth with no electron magnetic interference, no known health risks, security, and ubiquitous nature (can be used in RF-prohibited areas such as aircraft, space shuttles, and hospitals). In addition to the advantages over RF and IR-based communications, LEDs have more advantages than other light sources because of their faster switching time, high efficiency, smaller size, higher directivity, longer lifetime, and cheaper transmitter components compared to expensive RF units. Therefore, with all the advantages of visible light and LEDs, VLC systems is an attractive, alternative technology for indoor wireless communications^[1-4].

As LEDs are incoherent light sources, intensity modulation and direct detection (IM/DD) are used for data signals transmissions in VLC. The short carrier wavelength and large-area photo-detector lead to efficient Spatial Modulation (SM) that prevents fading. Nevertheless, at high data rates, e.g., beyond 10 Mbps, transmitted data signals become less immune to multipath dispersion(MPD), which results from the fact that data signals are received through line of sight as well as through reflections from walls and other objections in the room. MPD in turn causes inter-symbol interference(ISI) at the receiver^[5-6]. To overcome ISI, multicarrier modulation schemes like orthogonal frequency division multiplexing (OFDM) have been

proposed for OWC links^[7-8]. Optical OFDM(O-OFDM) signals designed for IM/DD systems must be real and non-negative. Two traditional unipolar OFDM schemes, namely DC-biased optical OFDM (DCO-OFDM), asymmetrically clipped optical OFDM (ACO-OFDM), have been proposed for OWC^[8-9]. In all two schemes, a real-value OFDM signal is obtained using the Hermitian symmetry condition. However, the two schemes use different methods to make the OFDM signal unipolar, i.e., real and nonnegative. In DCO-OFDM, a DC bias is added. In ACO-OFDM data symbols are allowed only on odd subcarriers. In addition, the negative parts of the OFDM signal are clipped off to obtain a unipolar signal. In the existing literature on optical OFDM with IM/DD, the research combines above two O-OFDM modulators with Spatial Modulation (SM) to result in a new method, namely Non-DC-biased OFDM (NDC-OFDM)^[10]. Compared to the conventional OSM-OFDM scheme combining traditional OSM with DCO-OFDM and ACO-OFDM, NDC-OFDM solves the DC-bias problem in DCO-OFDM and has a higher spectral efficiency than ACO-OFDM. However, NDC-OFDM system and conventional OSM-OFDM systems have deficiencies that can create high fluctuating envelopes which lead eye-safety problem, device lifetime problem and undesirable ambient lighting state problem.

In line with the above challenges, in this paper we propose a multicolor LEDs NDC-OFDM indoor VLC transmission scheme inheriting characteristics from SM(low complexity) and OFDM(ISI resistance). Instead of blue colored LEDs with wide-band phosphors, we choose multicolor LEDs to produce white light illumination. Since this solution offers the possibility for wavelength division multiplexing (WDM) which further increases overall transmission capacity. Most importantly, by merging Metameric

Modulation(MM) with Multicolor LEDs NDC-OFDM system in an appropriate way, it greatly makes high-speed data transmission with color control and maintaining constant perceived ambient lighting is possible. The new transmission scheme involving color gamut, frequency domain and spatial modulation three-dimension visible light resources multiplexing has not

been reported now, the overall structure is explained in more detail in Section 2.

1 Conventional OSM-OFDM system model

Within this section, DCO -OFDM and ACO -OFDM systems shown in Fig.1 are described in Section 1.1 and 1.2, and the transmission system

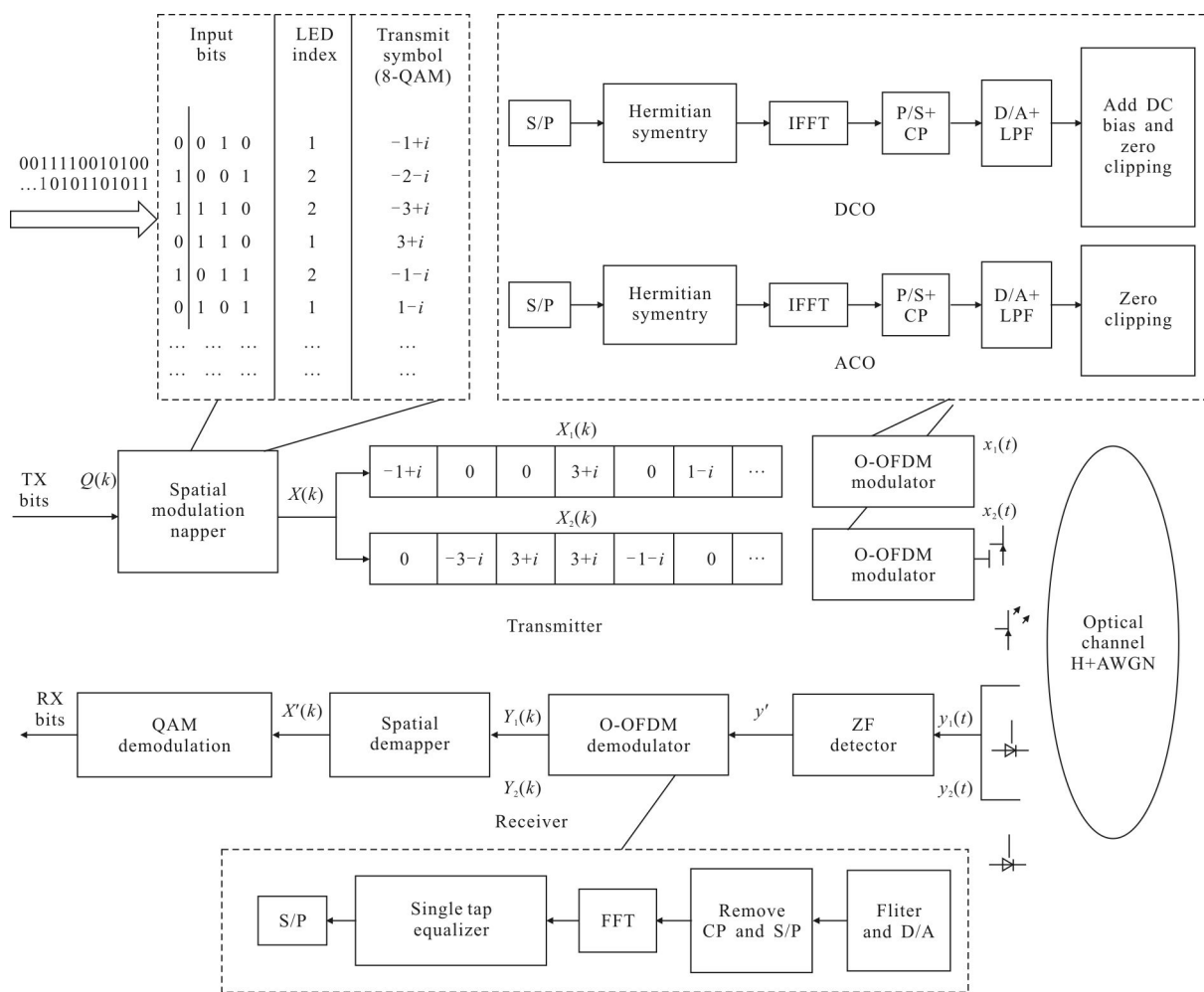


Fig.1 Block diagram of the conventional OSM-OFDM system

models for conventional OSM-OFDM is described in Section 1.3 in detail.

1.1 DCO-OFDM

A DCO-OFDM modulator with N subcarrier is taken into account N_{cp} is assumed to be the length of the OFDM cyclic prefix (CP). The complex data signal, $X=[X_0, \dots, X_{N-1}]$, is passed through the inverse fast Fourier transform (IFFT). Denote the IFFT value

of X by x , where $x=[x_0, \dots, x_{N-1}]$. The following IFFT computation is adopted^[8].

$$x_n = \frac{1}{\sqrt{N}} \sum_{k=0}^{N-1} X_k e^{j2\pi kn/N}, n=0, \dots, N-1 \quad (1)$$

The corresponding FFT computation is

$$x_k = \frac{1}{\sqrt{N}} \sum_{n=0}^{N-1} x_n e^{j2\pi kn/N}, k=0, \dots, N-1 \quad (2)$$

In order to make signal x is real-value not

complex, the following Hermitian symmetry condition can be used.

$$\begin{aligned} X_0 &= X_{N/2} = 0 \\ X_{N-k} &= X_k^*, \quad 0 \leq k \leq N/2 \end{aligned} \quad (3)$$

Due to the Hermitian symmetry condition in formula (3), the number of unique data carrying subcarriers presents in one DCO-OFDM symbol is $N/2 - 1$ M-QAM symbols. Signal x is then converted from parallel to serial (P/S), a cyclic prefix (CP) is appended, the resulting signal is passed through a digital-to-analog converter (D/A) and an ideal low pass filter (LPF) to obtain a continuous-time analog signal $x(t)$. Next, a suitable DC bias is added to $x(t)$ and any remaining negative peaks are clipped resulting in signal $x_{\text{DCO}}(t)$ that will be transmitted over the optical channel. The DC bias level is denoted by B_{DC} which is relevant to the standard deviation of $B_{\text{DC}}^{[11]}$.

$$B_{\text{DC}} = \mu \sqrt{E\{x(t)^2\}} \quad (4)$$

where μ is a proportionality constant, B_{DC} is defined as a bias of $10\log_{10}(\mu^2 + 1)$ dB.

1.2 ACO-OFDM

In ACO-OFDM, M-QAM symbols are transmitted on odd subcarriers only, while a bias signal is formed by the even subcarriers to ensure the transmitted OFDM signal is non-negative. Assuming that the input complex signal to IFFT block is X which comprises only odd components such that $X = [0, X_1, 0, X_3, \dots, X_{N-1}]$. Also, the elements of the vector X are constrained to have Hermitian symmetry as defined in formula (3). The resulting time domain signal, x , is real and has the antisymmetry property as defined below^[12]:

$$x_n = -x_{n+N/2}, \quad 0 \leq n \leq N/2 \quad (5)$$

The front-end of the ACO-OFDM transmitter is similar to a DCO-OFDM transmitter where x is first serialized and a CP is appended to it. Then x is D/A converted and sent across an ideal LPF resulting in the signal, $x(t)$. As negative samples cannot be conveyed in an IM/DD system, $x(t)$ is clipped at zero which results in the ACO-OFDM signal, $x_{\text{ACO}}(t)$. Due to the antisymmetry of x , clipping does not bring any loss of information. It's should be noted that one ACO-OFDM symbol carries $N/4$ M-QAM symbols instead of $N/2 - 1$ M-

QAM symbols as for DCO-OFDM.

1.3 Conventional OSM-OFDM System Model

The conventional OSM-OFDM system combines the SM with DCO-OFDM and ACO-OFDM two O-OFDM schemes. The system model is shown in Fig.1.

$Q(k)$ is an $n \times m$ binary matrix that will be transmitted in one OFDM symbol, where n is the number of OFDM subcarriers, and $m = \log_2(MN_t)$ is the number of bits that can be transmitted on each OFDM subchannel for the system uses a QAM constellation diagram of size M and N_t transmitters. Bits in the first column of SM mapping table shown in Fig.1 represent the LED index, the rest bits on the same row are converted to complex M-QAM symbols. This means that if the bit in the first column is zero, the M-QAM symbol on this row will be conveyed by the first LED, whereas the second LED is unactivated. In the same way, if the bit in the first column equals to one, the M-QAM symbol on this row will be conveyed by the second LED. Simultaneously, the first LED transmits zero power. Thus, only one LED is activated at any symbol duration. As a result of SM and M-QAM mapping, matrix $Q(k)$ is transformed into another complex matrix $X(k)$ of size $N_t \times n$. The complex matrix elements on each row are regarded as a row vector $X_t(k) (t=1, 2, \dots, N_t)$, and the length of the row vector is the number of OFDM subcarriers n . The symbols in this row vector $X_t(k)$ are the data that will be transmitted and from the transmitter t . Then, each row vector $X_t(k)$ is modulated using an O-OFDM modulator (e.g., DCO-OFDM, ACO-OFDM). The corresponding output O-OFDM signals, $x_1(t)$ and $x_2(t)$ will be fit for the optical multiple-input multiple-output (MIMO) channel transmission. For the analysis in this paper, it is sufficient to focus on the transmission of a single OFDM symbol.

Assuming that there is N_r PDs at the receiver, each PD converts optical signals to electrical signal (e.g., $y_1(t)$ and $y_2(t)$ in Fig.1). Additive white Gaussian noise(AWGN) is added to the electrical signals due to ambient light and thermal noise. It is assumed that the channel gain is known at the receiver in this paper

and the detection of transmitted symbols is based on Zero Force(ZF) principle defined as blow,

$$y'=H^{-1}y \quad (6)$$

where y' is an N_r dimension vector which is the corresponding estimated OFDM symbols sequence, H^{-1} denotes the inverse of the optical MIMO channel matrix $H_{N_r \times N_t}$, and y is $N_r \times n$ dimension received matrix. In this paper, both N_t and N_r are set to two.

After recovering corresponding estimated OFDM symbols sequence, y' is passed through the conventional O-OFDM demodulator block resulting in the matrix $Y(k)$ of size $N_r \times n$. Next, the receiver applied the spatial modulation detector to estimate the active LED index, at specific instant time k , as follows^[13].

$$g(k)=\operatorname{argmax}_i (Y(i,k)), i=1,\dots,N_t \quad (7)$$

where g is an $N_t \times n$ dimension matrix which contains all the estimated indexes. If $g(k)$ is equals to one, this means that the symbol received at the time instant k is transmitted from the first LED. On the contrary, if the result of $g(k)$ is two, the symbol is conveyed by the second LED. The formula (7) shows this process. After the SM demapper, $X'(k)$ is passed through the M-QAM demodulator to obtain the output bit stream.

$$X'(k)=\begin{cases} Y_1(k), & g(k)=1 \\ Y_2(k), & g(k)=2 \end{cases} \quad (8)$$

2 Multicolor LEDs NDC-OFDM indoor VLC system model

The proposed Multicolor LEDs NDC -OFDM system model is shown in Fig.2. We combine the

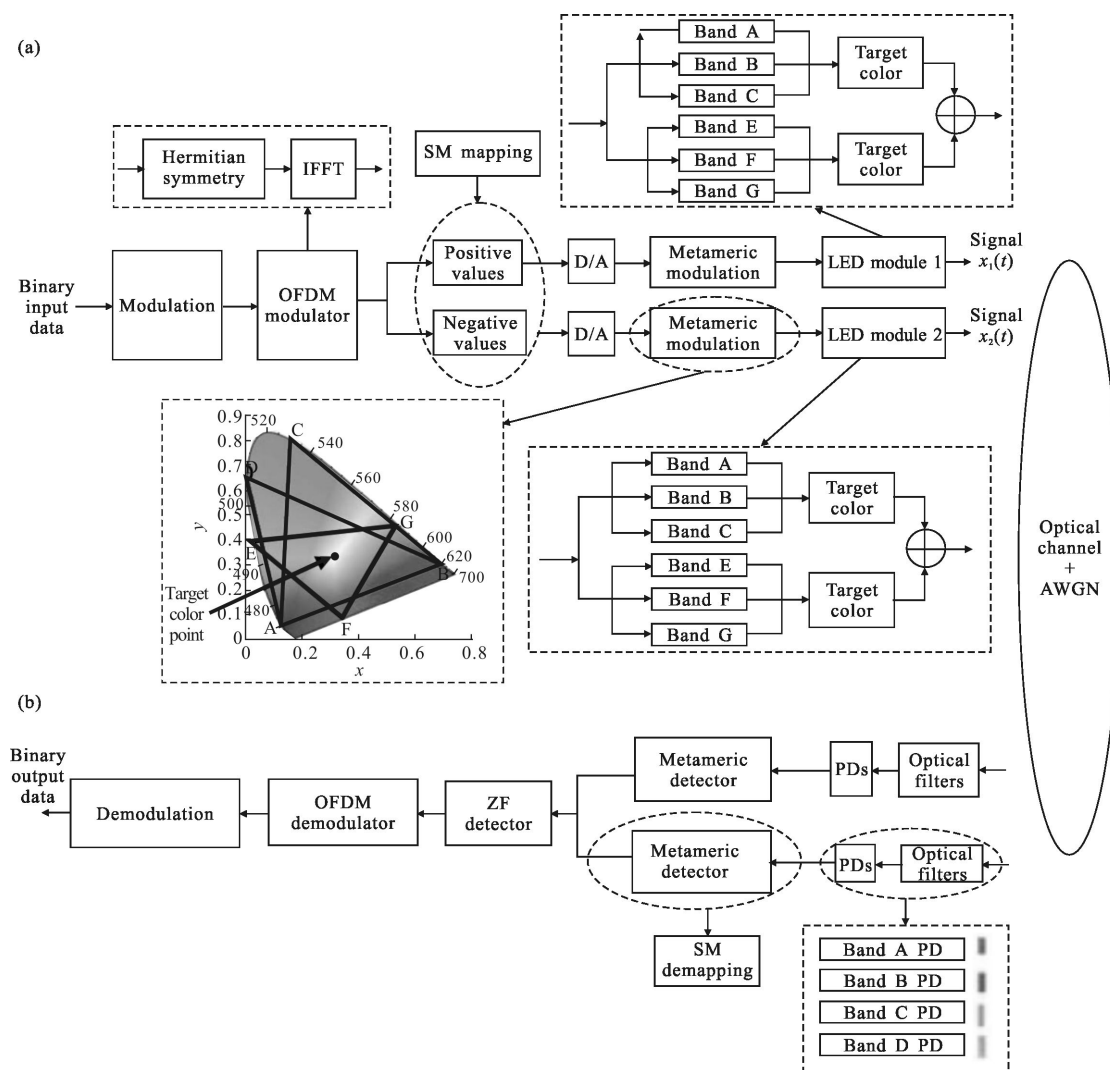


Fig.2 Complete system model for the Multicolor LEDs NDC-OFDM VLC system (a) transmitter and (b) receiver

NDC -OFDM and MM scheme together in the implementation of a multicolor LEDs indoor VLC system. The operation of the entire system is described as below.

2.1 Transmitter blocks

The transmitter mainly consists of modulation blocks, a SM mapping block, Metmeric modulation blocks, and LED modules. Several blocks within this transmitter are implemented as follows:

(1) Modulation: First, the binary input data is mapped to the specific modulation symbols. These symbols are then converted from serial to parallel, operated with Hermitian symmetry constrain condition, and inputted into the IFFT. The output signals of modulation blocks are real-value, but they are still bipolar.

(2) SM mapping: The real-value signals are divided into two channel signals by the SM mapping block. One channel conveys the positive signals, and the other channel transmits the absolute of the negative signals. The working principle is similar to the conventional OSM, and only one LED module is activated during one symbol time. If the transmitted symbol is positive, the first LED module will be activated to send the symbol. If the symbol is negative, its absolute value will be sent by the other LED module.

(3) Metameric modulation: The purpose of metameric modulation is to encode the data in the visible spectrum while maintaining a constant ambient lighting state. We use multiple primary sets each capable of generating its own color gamut. For example, we chose D sources and each primary is rendered with 3 elements of D sources, there are $(D, 3)$ possible primary sets. However we select only N of the possible primary sets so that the intersection of their color gamuts contain all of the desired lighting state. In this paper, we select $D=7$ and $D=3$. The three sets of primaries, [Blue, Green, Red], [Blue, Cyan, Red] and [Indigo, Pink, Yellow] have a significant overlap in their color gamuts. In this case

they are capable of generating a target point with three different metameric spectral power distribution (SPD).

(4) LED module: Centers of color bands A -F match with the seven primary colors Blue, Red, Cyan, Green, Indigo, Pink, Yellow in CIEUV color space. The color coordinates of seven primary colors are (0.169,0.007), (0.669,0.331), (0.135,0.8), (0.011,0.733), (0.025,0.4), (0.035,0.088) and (0.46,0.523), respectively. Three different primary colors combine an triangle that forms its own color gamut. The target color can be covered with three different color gamuts generated by three primary sets [Blue, Green, Red], [Blue, Cyan, Red] and [Indigo, Pink, Yellow], and the coordinate of the target color point is (0.35,0.32).

Assuming that the desired total intensity required to satisfy the ambient illumination or ambient brightness requirement is $C_T=3$, the maximum light intensity of each color LED is 1, and the inputted intensity to the LED module is C_i which has a relationship with the the output of the OFDM modulator. We chose the primary sets [Blue, Green, Red] and [Blue, Cyan, Red] which represent the positive-value signal and the negative-value signal, respectively, and the intensity of each corresponding LED is C_i . At the same time, we use another primary set, [Indigo, Pink, Yellow], to form the same target color, and the intensity of different color LED is $1-C_i$. The intention is used to compensate the constant ambient lighting intensity. The total output intensity of the LED module1 or the LED module2 always keeps 3. The intensity components of primary colors at the target color point is determined as follows.

The algorithm for the determination of intensities:

Step 1: Select a primary set among three given primary sets so that the target color point is located inside the triangle delimited by the corresponding color LEDs (denoted as A, B, and C in Fig.3);

Step 2: Draw a straight line from each LED through the target color point (line AD, BE and CF in Fig.3);

Step 3: Calculate the distance from the target color point to each LED point (d_1, d_3 and d_5 in Fig.3) and to the points of intersection (d_2, d_4 and d_6 in Fig.3) of the lines connecting the LED points;

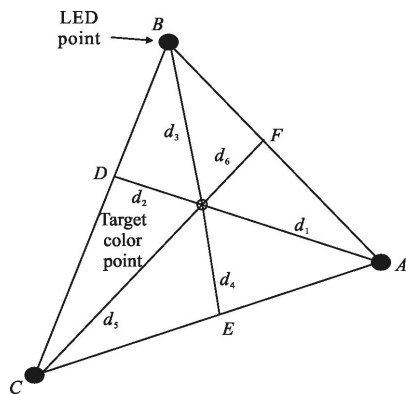


Fig.3 Calculation of LED intensities for the target color point

Step 4: According to the method of "the law of the lever" to calculate the intensity components^[14]. Since the intensity at any point on line BC depends only on the intensities of LED B and LED C, so the intensity of LED A at point D will be zero. Therefore, the intensity of LED A at target color point can be given by:

$$C_A = d_2 C_T / (d_1 + d_2) \quad (9)$$

Similarly, the intensities of LED B and LED C at target color point are obtained by Eqs. (11) and (12), respectively:

$$C_B = d_4 C_T / (d_3 + d_4) \quad (10)$$

$$C_C = d_6 C_T / (d_5 + d_6) \quad (11)$$

2.2 Receiver blocksc

Several blocks within the multicolor LEDs NDC-OFDM VLC receiver are implemented as follows:

(1) Optical filters and PDs: A PD combines with an optical narrow bandpass filter (OBPF) and an optical concentrator measures the intensity of each color. An ideal OBPF would have a completely flat passband and would completely block the remainder. Here we assumed four OBPFs, each passes light of the desired wavelength to the PDs. The PDs detect incident light intensities and the transmitted signals are obtained from two sets of received intensities.

(2) Metameric detector: Assuming that we have P PDs, and the corresponding PD spectral responses is

$S_p'(\lambda)$. $L_k^n(\lambda)$ is the individual emission spectra of the k th source from the n th set of primaries (it is assumed that we select $N=3$ sets of primaries each with $K=3$ sources). When light from all sources of the n th set of the primaries is incident on the p th PD, its output, I_p^n , is given by (12).

$$I_p^n = \sum_{k=1}^3 w_k \int_0^\infty L_k^n(\lambda) S_p'(\lambda) d\lambda \quad (12)$$

where w_k is the relative amount of each primary that is needed to achieve a metameral match with the spectral power distribution (SPD) of the ambient color. In this paper we assume that the SPD of the ambient color and the relative amount of each primary are known at the receiver.

For a given primary, every column of the response matrix R_g given by (13) would be distinct. Therefore, by comparing the output of the PDs with the column of R_g , the system can then detect which primary set is currently active. It should be noted that the primary set, [Indigo, Pink, Yellow], is merely used to maintain the constant ambient light intensity, and does not carry any data information. Hence, the response matrix R_g can be designed as below:

$$R_g = \begin{pmatrix} I_1^1 & \cdots & I_1^{N-1} \\ \vdots & \ddots & \vdots \\ I_p^1 & \cdots & I_p^{N-1} \end{pmatrix} \quad (13)$$

(3) ZF detector and SM detector: ZF block is used to reverse the impairments of the MIMO channel. The principle of ZF and SM detectors are identical with the two detectors of the conventional OSM-OFDM system shown in Fig.1.

(4) OFDM demodulator and demodulation: the processing of the OFDM demodulator is the same as a conventional OFDM receiver. The resultant symbols of the OFDM demodulator may be demodulated to produce the desired binary values.

3 Simulation results and discussions

This section presents numerical results on the

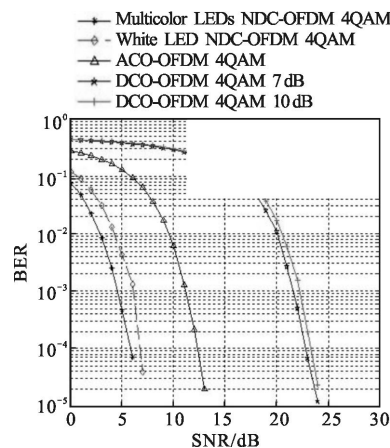
BER performance of conventional OSM-OFDM-VLC system and the proposed system for constellations such as 4-QAM, 16-QAM, 64-QAM and 256-QAM. We assume that the target color information can be accurately delivered to the receiver through a separate channel, such as a control channel. Table 1 lists the simulation parameters applied in the simulation experiments. The channel noise was assumed to be an Additive White Gaussian Noise (AWGN) caused by incandescent, fluorescent, and other background light that can interfere with the VLC signals. Although these noise can be minimized by optical filtering, still shot noise may exist in a well-designed receiver. Owing to its high intensity, this shot noise can also be modeled as White Gaussian Noise independently of the VLC signals. At the receiver, four PDs with different spectral distributions, combined with optical concentrators and four filters with different frequency band ranges, were used for light detection. A different responsivity problem in the PDs for different colors could be compensated by the LED driver circuit.

Tab.1 Simulation parameters

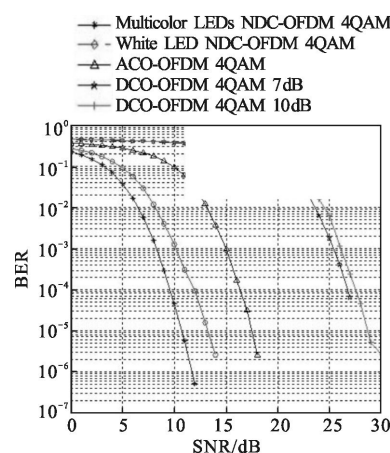
Parameters	Value
Number of LEDs	7
Number of PDs	4
Total intensity	3
Path loss between the LED modules and the PDs	$H=10^{-5} \times \begin{pmatrix} 0.1889 & 0.0713 \\ 0.0713 & 0.1889 \end{pmatrix}$
Seven primary color coordinates in CIE1931 color space chromaticity diagram	R:(0.669,0.331) G:(0.011,0.733) B:(0.169, 0.007) P:(0.035, 0.088) C:(0.135, 0.3) Y:(0.46, 0.523) I:(0.025, 0.4)
Target color point coordinate in CIE1931 color space chromaticity diagram	(0.35,0.32)

Figure 4 compares the BER performances of different OSM-OFDM-VLC transmission systems, such as multicolor LEDs NDC-OFDM, white LED NDC-OFDM, ACO-OFDM and DCO-OFDM with 7 dB, 10 dB for different constellations. It can be seen clearly that the BER performance of the novel proposed

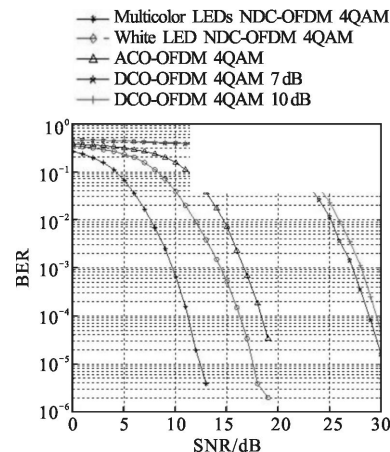
system outperforms the other three OSM-OFDM-VLC transmission systems for the same constellation. The curves of each subgraph depicted in Fig.4 have a good agreement with respect to the trends.



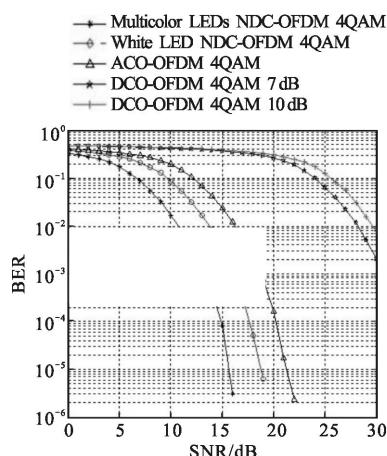
(a) OFDM-VLC transmission system performance for 4QAM constellation



(b) OFDM-VLC transmission system performance for 8QAM constellation



(c) OFDM-VLC transmission system performance for 16QAM constellation



(d) OFDM-VLC transmission system performance for 32QAM constellation

Fig.4 BER versus SNR of different OSM-OFDM-VLC transmission systems

In VLC, the compensation method by using pre-distortion of modulation input signal of LED might be considered to alleviate the performance degradation due to the large PAPR for OFDM signal^[15]. In this paper, we take the clipping operation to reduce the PAPR. In our proposed transmission system, we use the color rather than amplitude to represent the positive part and negative part of the OFDM signal. The main benefit of this approach is that although the noise induces the intensity fluctuation of the primary set, the color keeps constant anytime. It is the explanation that the proposed method is more resistant to signal clipping than other transmission schemes.

The definition of the bit error rate (BER) is the probability of occurrence of error of binary bit stream after system transmission. The ratio of signal average power to noise average power in the signal bandwidth is defined as signal-to-noise ratio (SNR). The BER curves for OFDM-VLC transmission systems with different clipping factors are depicted in Fig.5. As expected, the BER performance of the proposed scheme is smooth and better than ACO-OFDM for 32QAM constellation. Without forward error correction (FEC) coding, the latter requires 7 dB higher SNR than the former needs when the BER is 10^{-3} . It is also obvious that DCO-OFDM hardly yield a BER

below 10^{-3} without FEC coding, even if the SNR is improved greatly. In addition, the proposed transmission scheme starts exhibiting an error floor after SNR reaches 14 dB and 17 dB for two corresponding clipping level. When the clipping factor is 0.6, the proposed transmission scheme slightly outperforms white LED NDC-OFDM transmission system, and the BER performance reverses when the SNR exceeding 18.5 dB. This result comes from the fact the total intensity of proposed scheme is three times as larger as the white LED NDC-OFDM scheme, the clipping operation can't bring down the nonlinear distortion with the SNR increasing. Nevertheless, the proposed method may be provided with the superiority that it is capable of maintain the constant perceived ambient lighting while ensuring a reliable BER performance in comparison with other NDC-OFDM-VLC transmission systems.

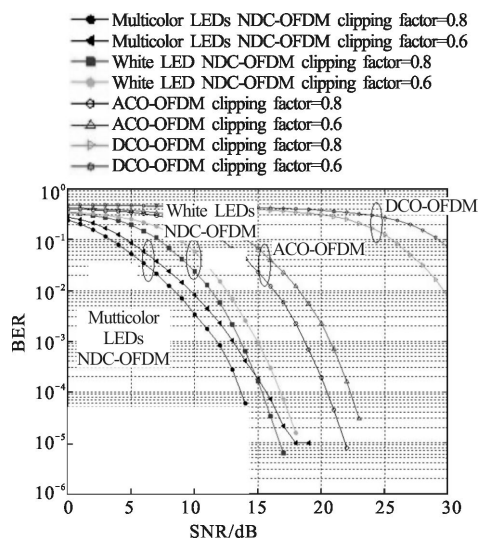


Fig.5 BER versus SNR of different OSM-OFDM-VLC transmission system for 32QAM constellation in respect of different clipping level

4 Conclusions

We proposed an multicolor LEDs NDC-OFDM-based VLC transmission scheme that is able to provide a more dependable BER performance and constant perceived ambient lighting simultaneously. To overcome nonlinear distortion caused by high PAPR

of signal, clipping operation is utilized. Through simulations, we have shown that the proposed NDC-OFDM VLC system not only can provide high-reliability transmission and high-robustness to high PAPR, but also doesn't have intensity fluctuation. Although LED module will enhance the implementation complexity in this novel case, recent advances in VLC technology have demonstrated that this inherent limitation can be solved presently. The proposed new complex solutions in this paper can become cost-effective and practical in a near future.

References:

- [1] Komine T, Nakagawa M. Fundamental analysis for visible-light communication system using LED lights [J]. *IEEE Transactions on Consumer Electronics*, 2004, 50(1): 50-100.
- [2] Grubor J, Gaeta J-O, Waleski J, et al. High-speed wireless indoor communication via visible light[J]. *ITG Fachbericht*, 2007, 198: 203-208.
- [3] Daz Pankaz, Youngil Park, Ki-Doo Kim. Performance of color-independent OFDM visible light communication based on color space[J]. *Optics Communications*, 2014, 324: 264-268.
- [4] Shen Zhenmin, Lan Tian, Wang Yun. Simulation and analysis for indoor visible-light communication based on LED [J]. *Infrared and Laser Engineering*, 2015, 44(8): 2496-2500.
- [5] Gfeller F R, Bapst U. Wireless in-house data communication via diffuse infrared radiation [J]. *Proceedings of the IEEE*, 1979, 67(11): 1474-1486.
- [6] Kahn J M, Barry J R. Wireless infrared communication[J]. *IEEE*, 1999, 85(2): 265-298.
- [7] Stefan I, Elgala H, Mesleh R, et al. Optical wireless OFDM system on FPGA: Study of LED nonlinearity effects [J]. *IEEE VTC Spring*, 2011: 1036-1042.
- [8] Armstrong J. OFDM for optical communication [J]. *J Lightwave Technol*, 2009, 27(3): 189-204.
- [9] Armstrong J, Schmidt B J C. Comparison of asymmetrically clipped optical OFDM and DC-biased optical OFDM in AWGN[J]. *IEEE Commun Lett*, 2008, 12(5): 343-345.
- [10] Li Yichen, Dobroslav Tsonev, Harald Haas. Non-DC-biased OFDM with optical spatial modulation [C]//2013 IEEE 24th International Symposium on Personal, Indoor and Mobile Radio Communication: Fundamentals and PHY Track, 2013: 486-490.
- [11] Sarangi Devasmitha Dissanayake, Jean Armstrong. Comparison of ACO-OFDM, DCO-OFDM and ADO-OFDM in IM/DD systems[J]. *Journal of Lightwave Technology*, 2013, 31(7): 1063-1072.
- [12] Asadzadeh K, Dabbo A, Hranilovic S. Receiver design for asymmetrically clipped optical OFDM [C]//IEEE GLOBECOM OWC Workshop, 2011.
- [13] Jeganathan J, Ghayeb A, Szczecinski L. Spatial modulation: optimal detection and performance analysis [C]//IEEE Communication Letters, 2008, 12(8): 545-547.
- [14] Nassau K. Color for Science, Art and Technology [M]. Holland: Elsevier, 1996.
- [15] Daechun Lee, Kyungmook Choi, Ki-Doo Kim, et al. Visible light wireless communications based on predistorted OFDM [J]. *Optics Communications*, 2012, 285 (7): 1767-1770.